Thymosin-β 4 induces angiogenesis in critical limb ischemia mice via regulating Notch/NF-κB pathway

SHUMIN LV[1], HONGWEN CAI[1], YIFEI XU[1], JIN DAI[1], XIQING RONG[1] and LANZHI ZHENG[2]

Departments of [1]Cardiovascular Medicine and [2]Emergency Internal Medicine,
The First Affiliated Hospital of Zhejiang Chinese Medical University, Hangzhou, Zhejiang 310006, P.R. China

Received December 30, 2019; Accepted June 22, 2020

DOI: 10.3892/ijmm.2020.4701

Abstract. Thymosin-β 4 (Tβ4) has been reported to exert a pro-angogenic effect on endothelial cells. However, little is known on the role and underlying mechanisms of Tβ4 on critical limb ischemia (CLI). The present study aimed therefore to investigate the mechanisms and pro-angiogenic effects of Tβ4 in CLI mice. Tβ4 overexpression lentiviral vector was first transfected into HUVEC and CLI mice model, and inhibitors of Notch pathway (DAPT) and NF-κB pathway (BMS) were also applied to HUVEC and CLI mice. Subsequently, MTT, tube formation and wound healing assays were used to determine the cell viability, angiogenesis and migratory ablity of HUVEC, respectively. Western blotting, reverse transcription, quantitative PCR, immunofluorescence and immunohistochemistry were used to detect the expression of the angiogenesis-related factors angiopoietin-2 (Ang2), TEK receptor tyrosine kinase 2 (tie2), vascular endothelial growth factor A (VEGFA), CD31 and α-smooth muscle actin (α-SMA) and the Notch/NF-κB pathways-related factors NOTCH1 intracellular domain (N1ICD), Notch receptor 3 (Notch3), NF-κB and p65 in HUVEC or CLI mice muscle tissues. The results demonstrated that Tβ4 not only enhanced the cell viability, angiogenesis and migratory ability of HUVEC but also promoted the expression of Ang2, tie2, VEGFA, N1ICD, Notch3, NF-κB, and phosphorylated (p)-p65 in HUVEC. In addition, Tβ4 promoted the expression of CD31, α-SMA Ang2, tie2, VEGFA, N1ICD and p-p65 in CLI mice muscle tissues. Treatment with DAPT and BMS had opposite effects of Tβ4, whereas Tβ4 reversed the effect of DAPT and BMS. The findings from the present study suggested that Tβ4 may promote angiogenesis in CLI mice via regulation of Notch/NF-κB pathways.

Correspondence to: Dr Lanzhi Zheng, Department of Emergency Internal Medicine, The First Affiliated Hospital of Zhejiang Chinese Medical University, 54 Youdian Road, Hangzhou, Zhejiang 310006, P.R. China
E-mail: lanzhi316@126.com

Abbreviations: Tβ4, thymosin-β 4; CLI, critical limb ischemia

Key words: thymosin-β 4, limb ischemia, angiogenesis, Notch, NF-κB

Introduction

Peripheral arterial disease results from progressive narrowing of arteries with a great impact on lower limb, which leads to critical limb ischemia (CLI) (1). Previous studies demonstrated that patients with peripheral arterial disease have a 40% increased risk of stroke and a 20-60% increased risk of myocardial infarction, and that patients with CLI in particular would have an additional substantial risk of limb loss (1,2). CLI is a gradual process in which arteries become blocked, narrowed or weakened (3). It is therefore crucial to develop novel therapeutic options for patients who develop CLI. In clinical, although some therapeutic strategies exist, including surgical or interventional revascularization, substantial number of patients are not eligible for those treatments and amputation can be the only option (4). Previous studies have reported that therapeutic neovascularization is a promising option that could overcome ischemia by providing an improved vascular network (4,5). However, the process of neovascularization is complex and involves the induction of capillary sprouting (angiogenesis), the maturation of newly formed vessels and the growth of large-conductance vessels (arteriogenesis) to improve blood supply (6-8).

Thymosin-β 4 (Tβ4) is a naturally-occurring peptide that is encoded in humans by the TMSB4X gene on the X-chromosome (9). Tβ4 is the most abundant and biologically active member of the β-thymosin family, which is presents in all body fluids and all cells, except from red blood cells (10). Tβ4 is the major G-actin-sequestering protein in mammalian cells and it prevents actin polymerization into filaments, confirming its crucial role in maintaining cytoskeletal dynamics (11). In the last decade, Tβ4 has been reported to possess the ability to regulate multiple biological functions. For example, Kobayash *et al* (12) have demonstrated that Tβ4 regulates the motility and metastasis abilities of mouse fibrosarcoma cells. Renga *et al* (13) have reported that Tβ4 can limit inflammation by regulating autophagy, and Kleinman and Sosne (14) have demonstrated that Tβ4 can promote dermal healing. In addition, previous studies reported that Tβ4 has the ability to regulate endothelial cell angiogenesis (10,15). Tβ4 has also been reported to promote the angiogenesis of endothelial progenitor cells, and Quan *et al* (16) showed that Tβ4 promotes the survival and angiogenesis of transplanted endothelial progenitor cells in infarcted myocardium. Furthermore, Zhao *et al* (17) demonstrated that Tβ4 can stimulate endothelial progenitor cell angiogenesis via a vascular endothelial growth factor-dependent mechanism. However, whether Tβ4 has a pro-angogenic effect in CLI needs to be further investigated and the underlying mechanisms must be determined. The present study aimed therefore to investigate the pro-angogenic effect and underlying mechanisms of Tβ4 in CLI mice.

Materials and methods

Ethics statement. All animal experiments were performed in accordance with the guidelines of the China Council on Animal Care and Use. This study was approved by the Committee of Experimental Animals of The First Affiliated Hospital of Zhejiang Chinese Medical University (approval no. Z20190312G). Every effort was made to minimize pain and discomfort to the animals. Animal experiments were performed in The First Affiliated Hospital of Zhejiang Chinese Medical University.

Cell culture. Human umbilical vein endothelial cells (HUVEC; cat. no. CRL-1730) and 293T/17 cells (cat. no. CRL-11268) were obtained from the American Type Culture Collection. HUVEC and 293T/17 cells were both cultured in DMEM (cat. no. C11995500BT; Gibco; Thermo Fisher Scientific, Inc.) containing 10% FBS (cat. no. 10437010; Gibco; Thermo Fisher Scientific, Inc.) and placed at 37˚C in a humidified incubator containing 5% CO_2. 293T/17 cells were only used for the construction of Tβ4 overexpression lentiviral. HUVEC were used for transfection and the MTT, tube formation, western blotting and immunofluorescence assays.

Construction of Tβ4 overexpression lentiviral vector. The sequence of the Tβ4 overexpression vector was as follows: Forward, 5'-TGGATTTGTACCATTCTTCTG-3' and reverse, 5'-GAAGAATGGTACAAATCCAAG-3' (Shanghai GenePharma Co., Ltd.). Once the overexpression sequence was ligated into pLJM1 plasmid vector (cat. no. 60908-4538; Tiandz, Inc.) by 2xEasyTaq SuperMix (cat. no. AS111-11; TransGen Biotech Co., Ltd.), 10 µl ligate product was mixed with 50 µl competent cell (*E.coli* DH5α; cat. no. MCC0010; Frdbio) and uniformly coated on the LB medium (cat. no. ST156; Beyotime Institute of Biotechnology). After the competent cell and LB medium were incubated for 16 h at 37˚C, the clone colonies were selected. Subsequently, plasmids were extracted using TIANprep Mini Plasmid Kit (cat. no. DP103-03; Tiangen Biotech Co. Ltd.). The pLJM1 plasmid vector without any target sequence was used as a negative control.

After collection of the Tβ4 overexpression plasmids, 293T/17 cells were placed into a 15 cm dish (1.2×10^7 cells in 20 ml complete medium) and were incubated at 37˚C overnight until confluence reached 20-30%. Subsequently, 100 ng overexpression plasmids and viral packaging plasmids psPAX2 (cat. no. VT1444; Youbio Technology Co., Ltd.) and pMD2.G (cat. no. VT1443; Youbio Technology Co., Ltd.) were co-transfected into 293T/17 cells using Lipofectamine 2000 (cat. no. 11668-019; Invitrogen; Thermo Fisher Scientific, Inc.). After 8 h, medium containing overexpression plasmids and viral packaging plasmids was replaced by fresh complete medium and cultured for another 48 h. The culture supernatant was then collected and centrifuged for 10 min at 4˚C (14,000 x g). The supernatant was filtered with 0.45 µm filter (cat. no. 342414; Beckman Coulter, Inc.), the lentiviral solution was centrifuged for 15 min at 4˚C (4,000 x g), the lentiviral vector was then concentrated, and the sample was finally collected and stored at -80˚C for subsequent experiments.

Lentiviral infection. Before infection, HUVEC were seeded into 6-well plates at the density of 1×10^6 cells in 2 ml complete medium and left in incubator overnight until confluence reached 20-30%. Subsequently, complete medium was replaced with serum-free DMEM and cells were cultured at 37˚C for 4 h. Subsequently, cells were infected with the Tβ4 overexpression lentiviral vector for 6 h. Medium containing lentiviral was replaced with complete medium and the cells were cultured for another 48 h at 37˚C.

DAPT and BMS treatment. The inhibitors of Notch pathway and of NF-κB pathway DAPT (cat. no. A8200) and BMS-345541 hydrochloride (BMS; cat. no. B4655), respectively, were obtained from APeXBIO Technology LLC. Following HUVEC infection with lentiviral vector, HUVEC were seeded into 6-well plates at the density of 1×10^6 cells in 2 ml complete medium and cultured until attachment. Then, DAPT and BMS were diluted in DMSO and cells were treated with 10 µM DAPT or 1 µM BMS for 48 h. The concentrations of DAPT and BMS were determined as previously described (18-20). Following treatment, cells were collected for further experiments.

MTT assay. MTT (cat. no. B7777; APeXBIO Technology LLC) assay was used to determine cell viability. Following HUVEC infection, cells were seeded into 96-well plates at the density of 1×10^4 cells in 100 µl complete medium. After 24 h, the cells were incubated with MTT reagent (0.5 mg/ml) for 4 h. MTT solution was discarded and 100 µl DMSO was added to each well. Finally, absorbance was detected at 570 nm on a microplate reader (Infinite M200 PRO; Tecan Group, Ltd.).

Tube formation assay. Following cell infection, HUVEC were diluted at the density of 2×10^5 cells in 200 µl medium and seeded into a 48 well plate which was precoated with 200 µl ECMatix gel (cat. no. ECM625; EMD Millipore). Cells were then incubated for 4 h. Subsequently, by using a phase-contrast optical microscope (Axio Lab.A1 pol; Leica Microsystems GmbH), series of tube-like structures were examined and photographed (magnification, x100).

Wound healing assay. Following cell infection, HUVEC were seeded into 6-well plates at a density of 3.5×10^5 cells in 2 ml of complete medium and cultured until confluence reached 95%. Then, a vertical wound in each well was created by using a 20 µl pipette tip, and medium was replaced by serum-free medium. Images in each well were collected at 0 and 48 h using a phase-contrast optical microscope (Axio Lab.A1 pol; magnification, x100). Image J software (version 1.8.0; National Institutes of Health) was used for data analysis.

Immunofluorescence. Following cell infection, HUVEC were fixed with 4% paraformaldehyde (cat. no. P804536, Macklin) for 15 min at room temperature and washed three times with PBS. Cells were permeabilized using 0.5% Triton X-100 in PBS (cat. no. R-10789704001; Roche Diagnostics) for 10 min at room temperature, washed three times with PBS and incubated overnight at 4˚C with NF-κB/p65 antibody (1:400; cat. no. 8242; Cell Signaling Technology, Inc.). The next day, cells were washed with PBS and incubated with Alexa Fluor 488 goat anti-rabbit IgG (1:1,000; cat. no. ab150077; Abcam) for 1 h at room temperature. Finally, cells were counterstained with 10 μg/ml DAPI (cat. no. D3571; Invitrogen; Thermo Fisher Scientific, Inc.) and visualized using a fluorescence microscope (CKX53; Olympus Corporation).

CLI model establishment. A total of 80 adult male C57BL/6J mice (8-weeks old) were obtained from Shanghai Laboratory Animal Technology. All animals were fed using the same animal feeding unit and given 12 h dark/12 h light cycle. Animals were maintained under specifc pathogen-free conditions at 20-25˚C and 50-65% humidity. Animals were randomly divided into eight groups (n=10/group) as follows: Sham, Model, negative control (NC), Tβ4, DAPT + NC, Tβ4 + DAPT, BMS + NC and Tβ4 + BMS groups. Before surgery, mice were intraperitoneally injected with ketamine (80 mg/kg; cat. no. 3131; R&D Systems, Inc.) and xylazine (10 mg/kg; cat. no. B27154; Yuanye). Once mice were anesthesized, 1 cm incision was made perpendicular to the right posterior inguinal ligament. Then, the proximal part of the right femoral artery and vein (including the superficial and deep branches, as well as the distal part of the saphenous artery and vein) was ligated and resected. The incision was sutured with propylene suture line (cat. no. LAT-18-5901; Lab Animal Technology Develop) (5). Finally, buprenorphine hydrochloride (0.1 mg/kg; cat. no. 2808; R&D Systems, Inc.) was injected subcutaneously to relieve postoperative pain. The mice were observed twice daily to monitor their health and behavior, and they did not appear to be in distress or to exhibit obvious behavioral abnormalities. On the 7th day following operation, mice were sacrificed with an overdose of pentobarbital sodium (100-150 mg/kg; intraperitoneally injected; cat. no. B005; Nanjing Jiancheng Bioengineering Institute), and the gastrocnemius muscle of the right hind limb was collected and stored at -80˚C for later use. The humane endpoints used in the study included the following: Animal death was verifed by the absence of pulse, breathing, corneal reflex and inaudibility of respiratory sounds and heartbeat sounds upon examination with a stethoscope.

For the Sham group, mice were only cut and the skin of a limb without ligation or resection was sutured. For the NC group, 14 days before the model establishment, mice were injected with $3x10^{12}$ NC lentiviral (10 times, 5 μl each time) into the right hind limb muscle during. For Tβ4 group, 14 days before the model establishment, mice were injected with $3x10^{12}$ Tβ4 overexpression lentiviral (10 times, 5 μl each time) vector into the right hind limb muscle. For the DAPT + NC and BMS + NC groups, based on the NC group and after the establishment of the model, mice were treated orally with 10 mg/kg BMS daily or intraperitoneally injected with 10 mg/kg DAPT daily for 7 days. For the Tβ4 + DAPT and Tβ4 + BMS groups, based on the Tβ4 group and after the establishment of the model, mice were intraperitoneally injected with 10 mg/kg DAPT or treated orally with 10 mg/kg BMS for 7 days. The concentrations of DAPT and BMS were determined according to previous studies (19,21,22).

Western blotting. HUVEC and animal samples were lysed using RIPA lysis buffer (cat. no. P0013B; Beyotime Institute of Biotechnology). Protein concentration was determined using a BCA assay kit (cat. no. 23250; Pierce; Thermo Fisher Scientific, Inc.). Proteins (30 μg) were separated by 10% SDS-PAGE (cat. no. P0052A; Beyotime Institute of Biotechnology) and transferred onto nitrocellulose membranes (cat. no. HTS112M: EMD Millipore). Membranes were blocked with 5% skimmed milk for 2 h at room temperature and incubated with primary antibodies against Ang2 (1:1,000; 57 kDa; cat. no. ab155106; Abcam), tie2 (1:1,000; 126 kDa; ab24859; Abcam), VEGF-A (1:1,000; 23 kDa; cat. no. ab46154; Abcam), N1ICD (1:500; 80 kDa; ab8925; Abcam), p-p65 (1:2,000; 70 kDa; cat. no. ab86299; Abcam), p65 (1:1,000; 64 kDa; cat. no. ab16502; Abcam), Notch3 (1:1,000; 270 kDa; cat. no. 2889; Cell Signaling Technology, Inc.) and GAPDH (1:1,000; 37 kDa; cat. no. 5174; Cell Signaling Technology, Inc.) at 4˚C overnight. The next day, membranes were incubated with HRP-conjugated goat anti-rabbit IgG secondary antibody (1:5,000; cat. no. ab205718; Abcam) for 1 h at room temperature. Bands were detected using SuperSignal West Pico Chemiluminescent Substrate (cat. no. 34078; Thermo Fisher Scientific, Inc.). Relative expression of various proteins was normalized to endogenous control GAPDH using Image Lab™ Software (version 3.0; Bio-Rad Laboratories, Inc.).

RNA extraction and reverse transcription quantitative (RT-q) PCR. mRNA was extracted from cells and gastrocnemius muscle samples using TRIzol (cat. no. 15596; Invitrogen; Thermo Fisher Scientific, Inc.) and collected into a 1.5 ml centrifuge tube (cat. no. 615001; Nest). Chloroform (160 μl; cat. no. C805334; Shanghai Macklin Biochemical Co., Ltd.) was added into the tube that was centrifuged at 4˚C for 20 min (14,000 x g). The supernatant was collected and mixed with an equal volume of isopropanol (cat. no. H822173; Shanghai Macklin Biochemical Co., Ltd.) and the samples were centrifuged at 4˚C for 5 min (14,000 x g). RNA sediment was diluted using RNase-free H_2O. Then, PrimeScript RT kit (cat. no. RR037A; Takara Bio, Inc.) was used to reverse-transcribe RNA into cDNA according to the manufacturers' instructions. Gene expression was tested by q-PCR assays using Verso 1-step RT-qPCR Kit (cat. no. A15300; Thermo Fisher Scientific, Inc.) in ABI 7500 Fast Real-Time PCR System (Applied Biosystems). RT-qPCR reactions were performed as follows: 95˚C for 30 sec, 60˚C for 30 sec, 45 cycles at 60˚C for 30 sec. The relative expression levels were normalized to endogenous control using $2^{-\Delta\Delta Cq}$ method (23). The sequences of the primers are presented in Table I (Sangon Biotech Co., Ltd.).

Table I. Sequences of the primers used for reverse transcription-quantitative PCR.

Target gene	Forward primers, 5'-3'	Reverse primers, 5'-3'
Ang2-human	AACTTTCGGAAGAGCATGGAC	CGAGTCATCGTATTCGAGCGG
Ang2-rat	AGAATAAGCAAGTCTCGCTTCC	TGAACCCTTTAGAGGCTCGGT
Tie2-human	TTAGCCAGCTTAGTTCTCTGTGG	AGCATCAGATACAAGAGGTAGGG
Tie2-rat	CAGCTTGCTCCTTTATGGAGTAG	ATCAGACACAAGAGGTAGGGAAT
VEGFA-human	AGGGCAGAATCATCACGAAGT	AGGGTCTCGATTGGATGGCA
VEGFA-rat	CTGCCGTCCGATTGAGACC	CCCCTCCTTGTACCACTGTC
GAPDH-human	GGAGCGAGATCCCTCCAAAAT	GGCTGTTGTCATACTTCTCATGG
GAPDH-rat	AGGTCGGTGTGAACGGATTTG	GGGGTCGTTGATGGCAACA

Immunohistochemistry. The density of capillaries ($CD31^+$ cells) and arterioles (α-SMA^+ cells) was observed by immunohistochemistry. After mice gastrocnemius muscle tissues were paraffin-embedded, the muscle tissues were placed on a microtome (cat. no. RM2235; Leica Microsystems GmbH) and cut into 4 μm thick slices. Then the slices were fixed 4% paraformaldehyde for 10 min at room temperature and placed on a glass slide (cat. no. 80302-3101-16-P4; ShiTai) and followed by deparaffinization (in two successive xylene baths) for 10 min. Following slides incubation with antigen repair solution (cat. no. p0081; Beyotime Institute of Biotechnology) for 10 min at room temperature, slides were incubated with endogenous peroxidase blocker (cat. no. BF06060; Biodragon Immunotech) for 10 min at room temperature. Tissue slides were blocked with 5% FBS (cat. no. 10437010; Gibco; Thermo Fisher Scientific, Inc.) for 1 h at room temperature. Slides were incubated with primary antibodies against CD31 (cat. no. ab134168; 1:500; Abcam) and α-SMA (cat. no. ab32575; 1:500; Abcam) overnight at 4˚C. Then, all sections were incubated with a secondary antibody (cat. no. G-21234; 1:500; Thermo Fisher Scientific, Inc.) at 37˚C for 30 min and treated with the DBA reagent (cat. no. SFQ004; Beijing 4A Biotech Co., Ltd.) for 30 min. Sections were treated with hematoxylin (cat. no. B25380; Yuanye) for 10 min and sealed with resin (cat. no. G8590; Beijing Solarbio Science & Technology Co., Ltd.). Finally, the capillaries density ($CD31^+$ cells) and arterioles density (α-SMA^+ cells) were observed and imaged using a phase-contrast optical microscope (Axio Lab.A1 pol; magnification, x400). Furthermore, immunohistochemistry quantification was evaluated by calculating the ratio of positive cell number to the total cell number in five fields, which were selected in each slide randomly.

Statistical analysis. Student's t-test and one-way ANOVA followed by Tukey's post-hoc test were used for statistical analysis. Data were analyszed using SPSS software (version 18.0, SPSS, Inc.). Data were presented as the means ± standard deviation. All experiments were conducted three times. P<0.05 was considered to indicate a statistically significant difference.

Results

Tβ4 promotes cell viability, angiogenesis and migration of HUVEC. Following Tβ4 overexpression in HUVEC, the transfection efficiency was detected by RTq-PCR, and MTT, tube formation and wound healing assays were conducted. As presented in Fig. 1A, Tβ4 expression level was increased in the Tβ4 group compared with NC group (P<0.001). Furthermore, Tβ4 overexpression significantly increased HUVEC viability compared with the NC group (Fig. 1B; P<0.05). In addition, Tβ4 enhanced the HUVEC angiogenesis (Fig. 1C) and migratory ability (Fig. 1D), compared with the NC group (both P<0.001).

Tβ4 promotes the expression of angiogenesis-related and Notch/NF-κB pathway-related factors in HUVEC. The expression of some angiogenesis-related factors were detected by western blottong and RTq-PCR. As presented in Fig. 2A and B, Tβ4 significantly upregulated the expression of Ang2, tie2 and VEGF-A at both translation and transcription levels, compared with the NC group (all P<0.001). Furthermore, whether the effect of Tβ4 on HUVEC angiogenesis was associated with Notch/NF-κB signaling pathway was evaluated. Western blotting and immunofluorescence were used to detect the expression of key proteins of Notch/NF-κB pathways. As presented in Fig. 2C, the protein expression of N1ICD and Notch3 was increased by Tβ4 group compared with NC group (P<0.001 and P<0.01, respectively). In addition, Tβ4 increased the expression of NF-κB/p65 in HUVEC nucleus (Fig. 2D). These results indicated that the effect of Tβ4 on HUVEC angiogenesis may be associated with Notch/NF-κB signaling pathway.

The promotion effects of Tβ4 on HUVEC viability and on N1ICD and p-p65 expression are mediated by Notch/NF-κB pathway. The inhibitors of Notch and NF-κB pathways (DAPT and BMS, respectively) were used in the present study. As presented in Fig. 3A, the expression of N1ICD and p-p65, as well as the ratio p-p65/p65 were significantly increased by Tβ4, but were decreased following treatment with DAPT and BMS compared with NC group (P<0.001, P<0.01 and P<0.05, respectively). Furthermore, in Tβ4 + DAPT and Tβ4 + BMS groups, the promotion effect of Tβ4 on the expression of theses proteins was reversed by treatment with DAPT and BMS compared with Tβ4 and DAPT + NC or BMS + NC groups (P<0.05 and P<0.001, respectively). Similarly, as presented in Fig. 3B, the promotion effect of Tβ4 on HUVEC viability was reversed by DAPT and BMS compared with Tβ4 and DAPT + NC or BMS + NC groups (P<0.05 and P<0.01, respectively). These results demonstrated that the promotion effects of Tβ4 on HUVEC viability

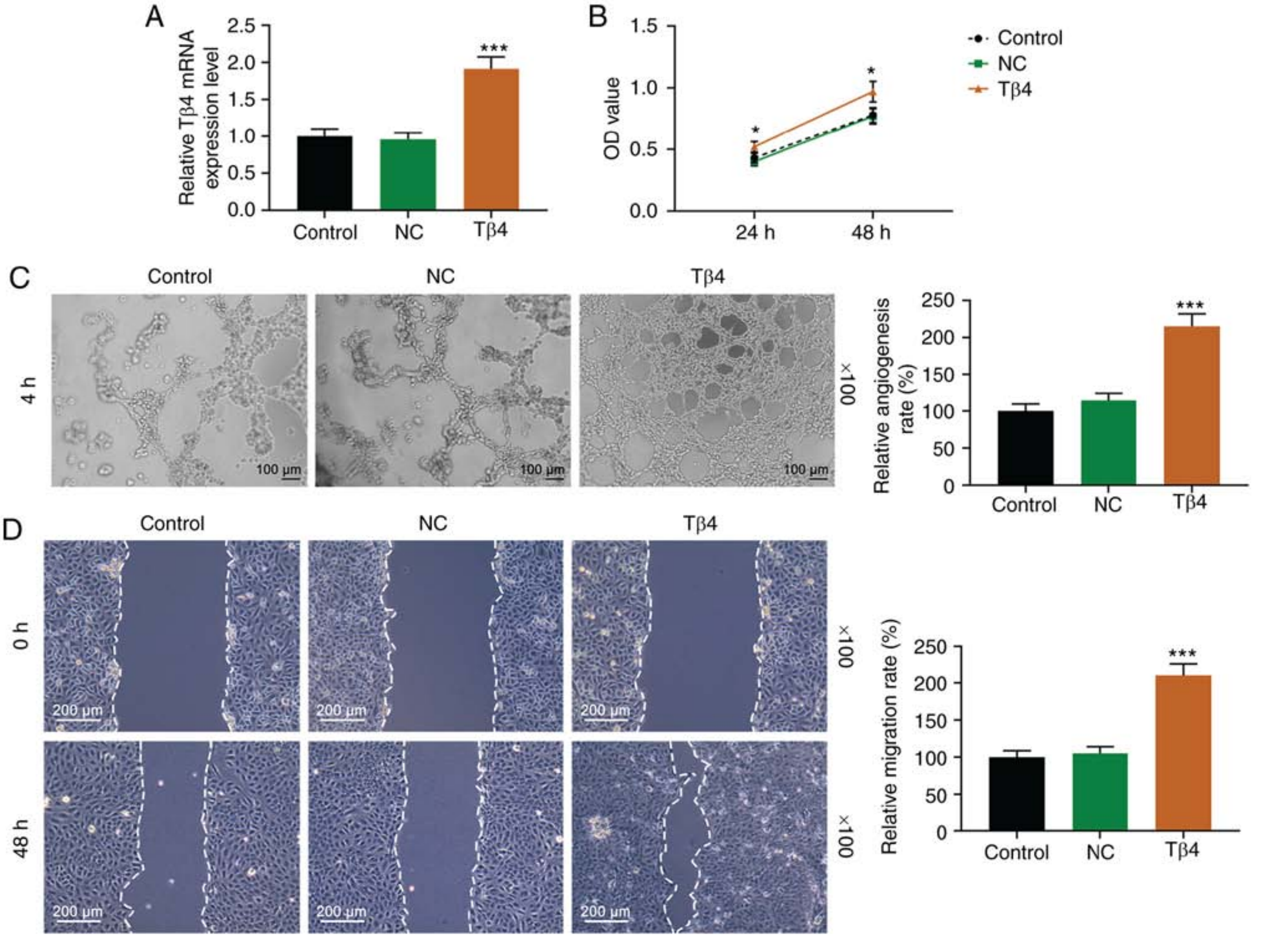

Figure 1. Tβ4 promoted cell viability, angiogenesis and migratory ability of HUVEC. (A) Tβ4 mRNA expression was detected by reverse transcription quantitative PCR after infection with Tβ4 overexpression lentiviral. (B) Viability of HUVEC was measured using MTT assays after infection with Tβ4 overexpression lentiviral. (C) Angiogenesis of HUVEC was measured using tube formation assay after infection with Tβ4 overexpression lentiviral vector. Magnification, x100. (D) Migratory ability of HUVEC was measured using wound healing assay after infection with Tβ4 overexpression lentiviral vector. (Magnification x100). All experiments were conducted three times. *P<0.05 and ***P<0.001 vs. NC. Tβ4, thymosin-β 4; NC, negative control; OD, optical density.

and N1ICD and p-p65 expression may be mediated by Notch/NF-κB signaling pathway.

The promotion effects of Tβ4 on HUVEC angiogenesis and migratory ability are mediated by Notch/NF-κB pathway. Regarding the effect of Tβ4 on HUVEC angiogenesis and migratory ability (Fig. 4A and B), the results demonstrated that the relative angiogenesis and migration rates of HUVEC were significantly increased by Tβ4 but were decreased following treatment with DAPT and BMS compared with the NC group (P<0.001, P<0.01 and P<0.05, respectively). Furthermore, in Tβ4 + DAPT and Tβ4 + BMS groups, the promotion effects of Tβ4 on HUVEC angiogenesis and migratory ability was reversed by DAPT and BMS treatments compared with Tβ4 and DAPT + NC or BMS + NC groups (P<0.05 and P<0.001, respectively). These results suggested that the promotion effects of Tβ4 on HUVEC angiogenesis and migratory ability may be mediated by Notch/NF-κB signaling pathway.

The promotion effects of Tβ4 on the expression of angiogenesis-related factors are mediated by Notch/NF-κB pathway. The changes in angiogenesis-related protein expression were detected following HUVEC treatment with DAPT and BMS. As presented in Fig. 5A and B, the protein and gene expression of Ang2, tie2 and VEGF-A were significantly increased by Tβ4 but were decreased following cell treatment with DAPT and BMS compared with the NC group (P<0.001 and P<0.01, respectively). Furthermore, in Tβ4 + DAPT and Tβ4 + BMS groups, the promotion effects of Tβ4 on the expression of these proteins were reversed by DAPT and BMS treatments compared with Tβ4 and DAPT + NC or BMS + NC groups (P<0.05, P<.01, and P<0.001, respectively). These findings further suggested that the promotion effects of Tβ4 on HUVEC angiogenesis and migratory ability were mediated by Notch/NF-κB signaling pathway.

Tβ4 enhances the capillary and arteriolar densities through regulating Notch/NF-κB pathway in CLI mice. In order to confirm the pro-angiogenesis effect of Tβ4, *in vivo* experiments were preformed. The expression of Tβ4 was increased in the Tβ4 group compared with NC group in gastrocnemius of right hind limb tissues (Fig. 5C; P<0.001). Once CLI mice model was established, the capillary and arteriolar densities were observed by immunohistochemical

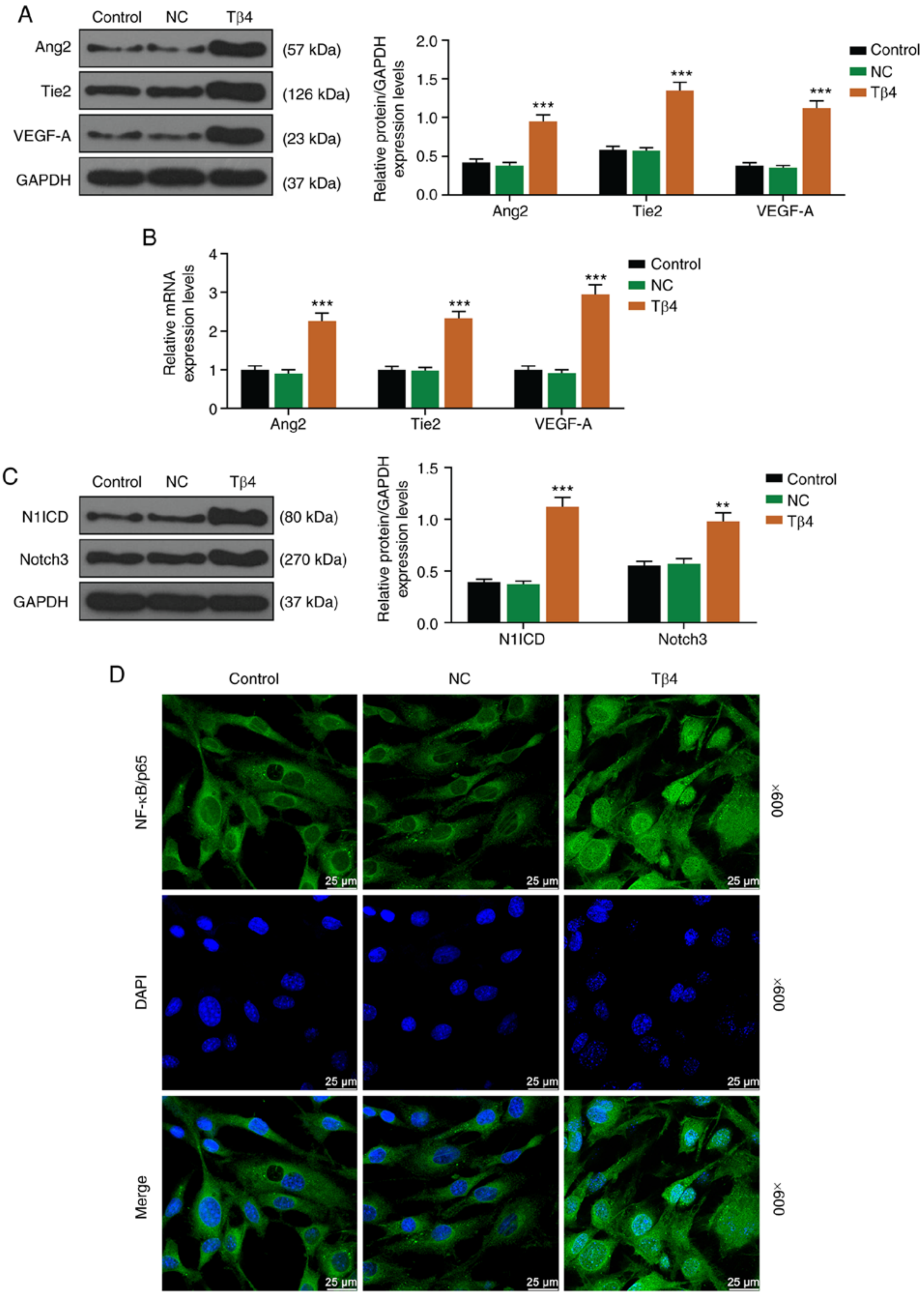

Figure 2. Tβ4 promoted the expression of angiogenesis-related and Notch/NF-κB pathway-related proteins in HUVEC. (A) Protein expression of Ang2, tie and VEGF-A were detected by western blotting after infection with Tβ4 overexpression lentiviral. GAPDH was used as an internal control. (B) mRNA expression of Ang2, tie2 and VEGF-A were detected by reverse transcription quantitative PCR after infection with Tβ4 overexpression lentiviral vector. GAPDH was used as an internal control. (C) Protein expression of N1ICD and Notch3 were detected by western blotting after infection with Tβ4 overexpression lentiviral vector. GAPDH was used as an internal control. (D) Expression of NF-κB/p65 in HUVEC nucleus was detected by immunofluorescence. Magnification, x600. All experiments were conducted three times. **P<0.01 and ***P<0.001 vs. NC. VEGF-A, vascular endothelial growth factor A; Ang2, angiopoietin-2; tie2, tyrosine kinase 2; NC, negative control; N1ICD, NOTCH1 intracellular domain; Notch3, Notch receptor 3; Tβ4, thymosin-β 4.

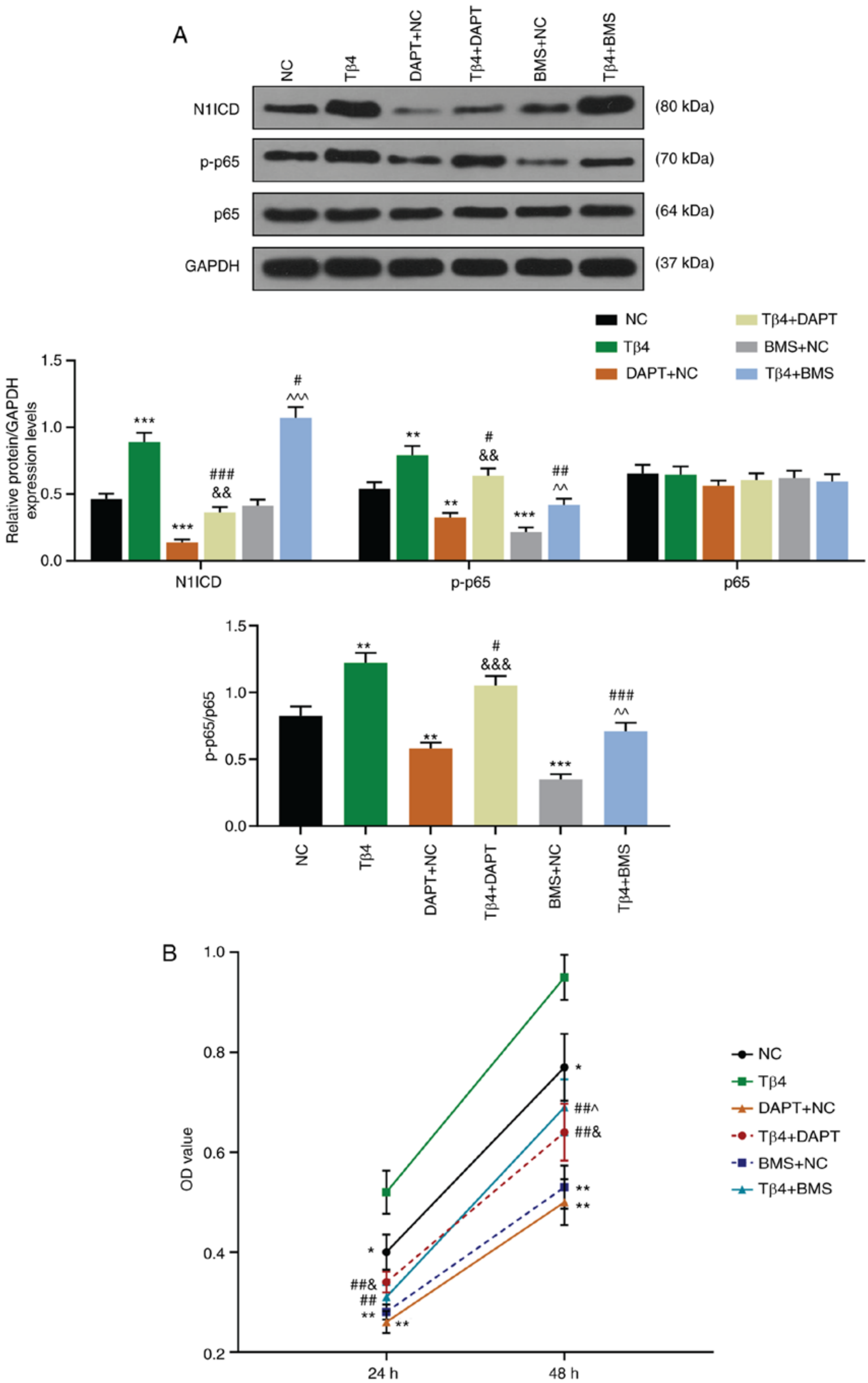

Figure 3. Promotion effects of Tβ4 on HUVEC viability and N1ICD and p-p65 expressions were mediated by Notch/NF-κB signaling pathway. (A) Protein expression of N1ICD and p-p65 were detected by western blotting after infection with Tβ4 overexpression lentiviral and treatment with DAPT or BMS. GAPDH was used as an internal control. (B) Viability of HUVEC was measured using MTT assay after infection with Tβ4 overexpression lentiviral vector and treatment with DAPT or BMS. All experiments were conducted three times. $^{*}P<0.05$, $^{**}P<0.01$ and $^{***}P<0.001$ vs. NC; $^{\#}P<0.05$, $^{\#\#}P<0.01$ and $^{\#\#\#}P<0.001$ vs. Tβ4; $^{\&\&}P<0.05$ and $^{\&\&\&}P<0.001$ vs. DAPT + NC; $^{\wedge\wedge}P<0.05$ and $^{\wedge\wedge\wedge}P<0.001$ vs. BMS + NC. NC, negative control; N1ICD, NOTCH1 intracellular domain; Tβ4, thymosin-β 4; p-, phosphorylated.

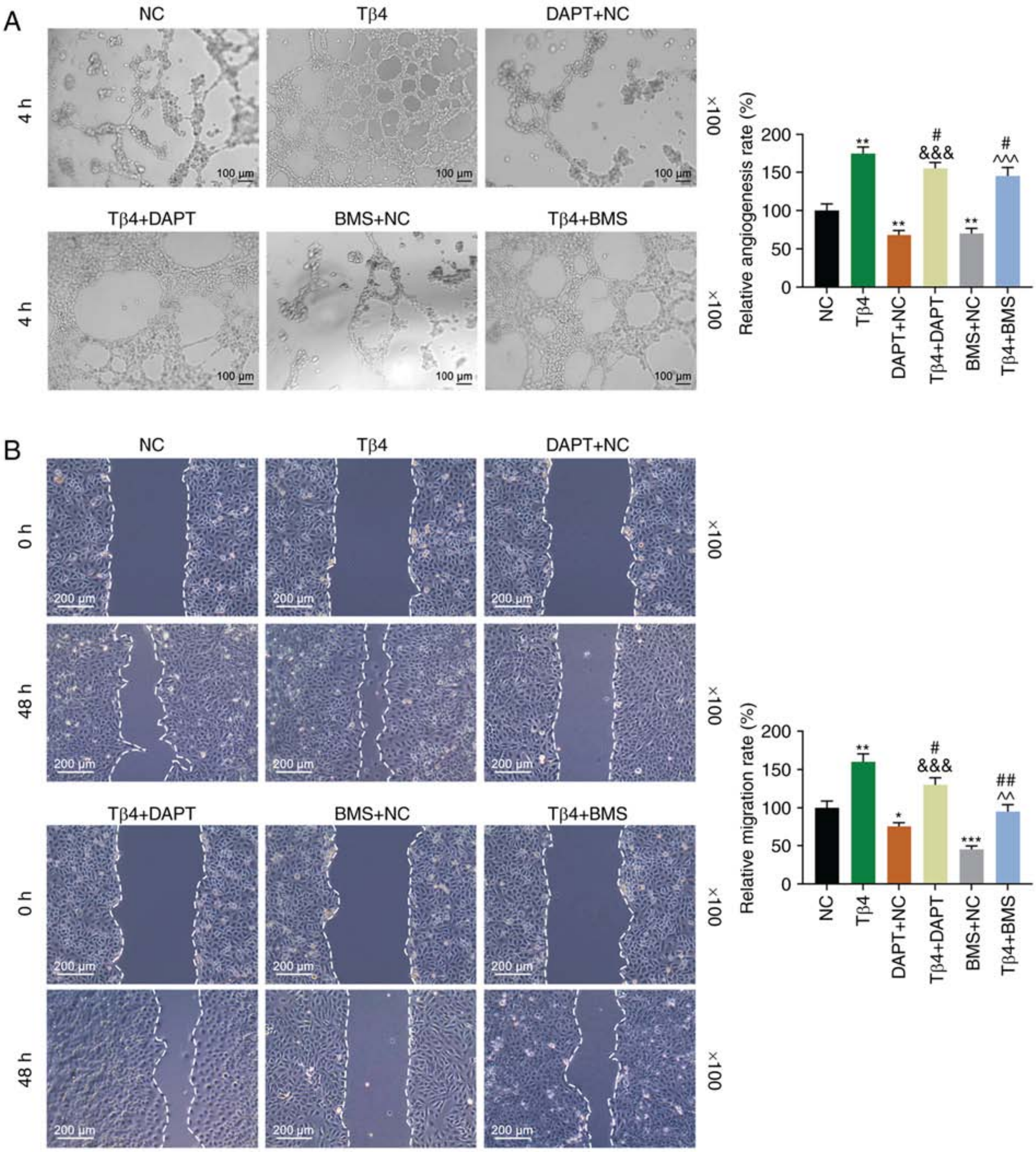

Figure 4. Promotion effects of Tβ4 on HUVEC angiogenesis and migratory ability were mediated by Notch/NF-κB signaling pathway. (A) Angiogenesis of HUVEC was measured using tube formation assay after infection with Tβ4 overexpression lentiviral vector and treatment with DAPT or BMS. (Magnification, x100). (B) Migratory ability of HUVEC was measured using wound healing assay after infection with Tβ4 overexpression lentiviral vector and treatment with DAPT or BMS. (Magnification, x100). All experiments were conducted three times. *P<0.05, **P<0.01 and ***P<0.001 vs. NC; #P<0.05 and ##P<0.01 vs. Tβ4; &&&P<0.001 vs. DAPT + NC; ^^P<0.001 and ^^^P<0.001 vs. BMS + NC. NC, negative control; Tβ4, thymosin-β 4.

staining. As presented in Fig. 6A and B, capillary density ($CD31^+$ cells) and arteriolar density (α-SMA^+ cells) were remarkably decreased in Model, NC, DAPT + NC, and BMC + NC groups, but were increased in Tβ4 group. Furthermore, in Tβ4 + DAPT and Tβ4 + BMS groups, the promotion effects of Tβ4 on the densities of capillary and arteriolar were reversed by DAPT and BMS treatment. These results demonstrated that Tβ4 may have the ability to increase capillary and arteriolar densities in CLI mice, and that these effects might be mediated by Notch/NF-κB signaling pathway.

Tβ4 enhances the expression of angiogenesis-related proteins by regulating Notch/NF-κB pathway in CLI mice. To further verify the current findings, the expression of angiogenesis-related proteins was detected in CLI mice. As presented in Fig. 7A and B, the protein and gene expression of Ang2, tie2 and VEGF-A were significantly increased by Tβ4, but were decreased following treatment with DAPT and BMS compared with the NC group (P<0.001 and P<0.05, respectively). Furthermore, in Tβ4 + DAPT and Tβ4 + BMS groups, the promotion effects of Tβ4 on the expression of these proteins were reversed by DAPT and BMS treatment, compared with

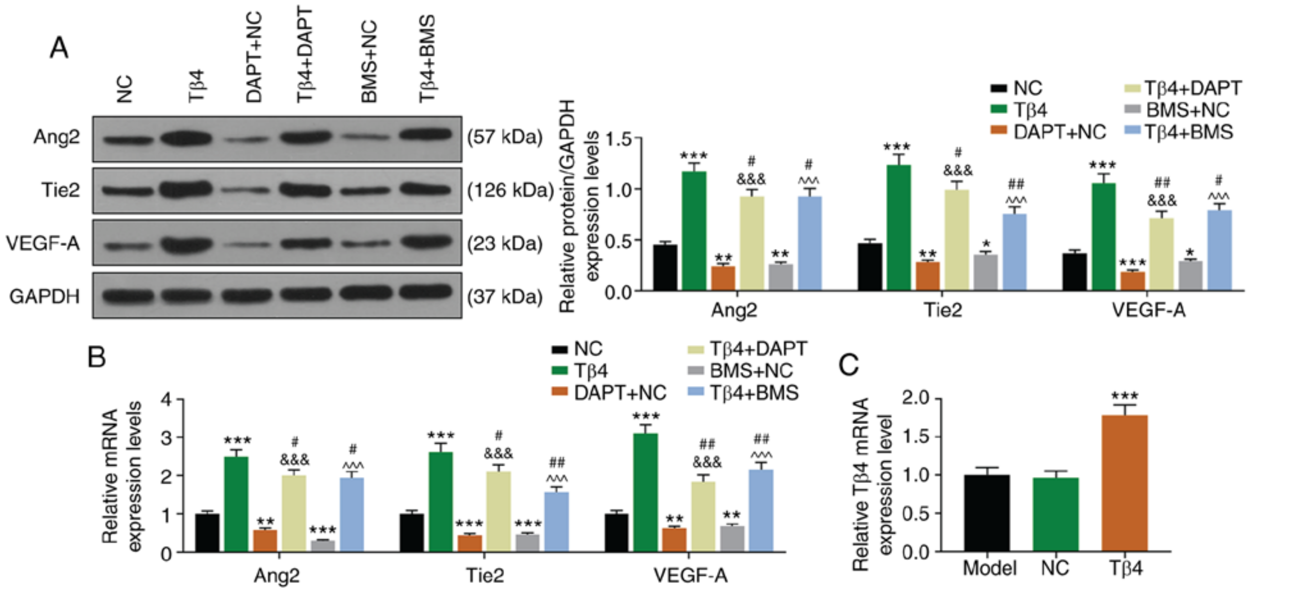

Figure 5. Promotion effects of Tβ4 on the expression of angiogenesis-related proteins were mediated by Notch/NF-κB signaling pathway. (A) Protein expression of Ang2, tie2 and VEGF-A were detected by western blotting after infection with Tβ4 overexpression lentiviral vector and treatment with DAPT or BMS. GAPDH was used as an internal control. (B) mRNA expression of Ang2, tie2 and VEGF-A was detected by reverse transcription quantitative PCR after transfected with Tβ4 and treatment with DAPT or BMS. GAPDH was used as an internal control. (C) mRNA expression of Tβ4 was detected in CLI mice muscle tissues. All experiments were conducted three times. *P<0.05, **P<0.01 and ***P<0.001 vs. NC; $^{\#}$P<0.05 and $^{\#\#}$P<0.01 vs. Tβ4; $^{\&\&\&}$P<0.001 vs. DAPT + C; $^{\wedge\wedge\wedge}$P<0.001 vs. BMS + NC. VEGF-A, vascular endothelial growth factor A; Ang2, angiopoietin-2; tie2, tyrosine kinase 2; NC, negative control; Tβ4, thymosin-β 4; CLI, critical limb ischemia.

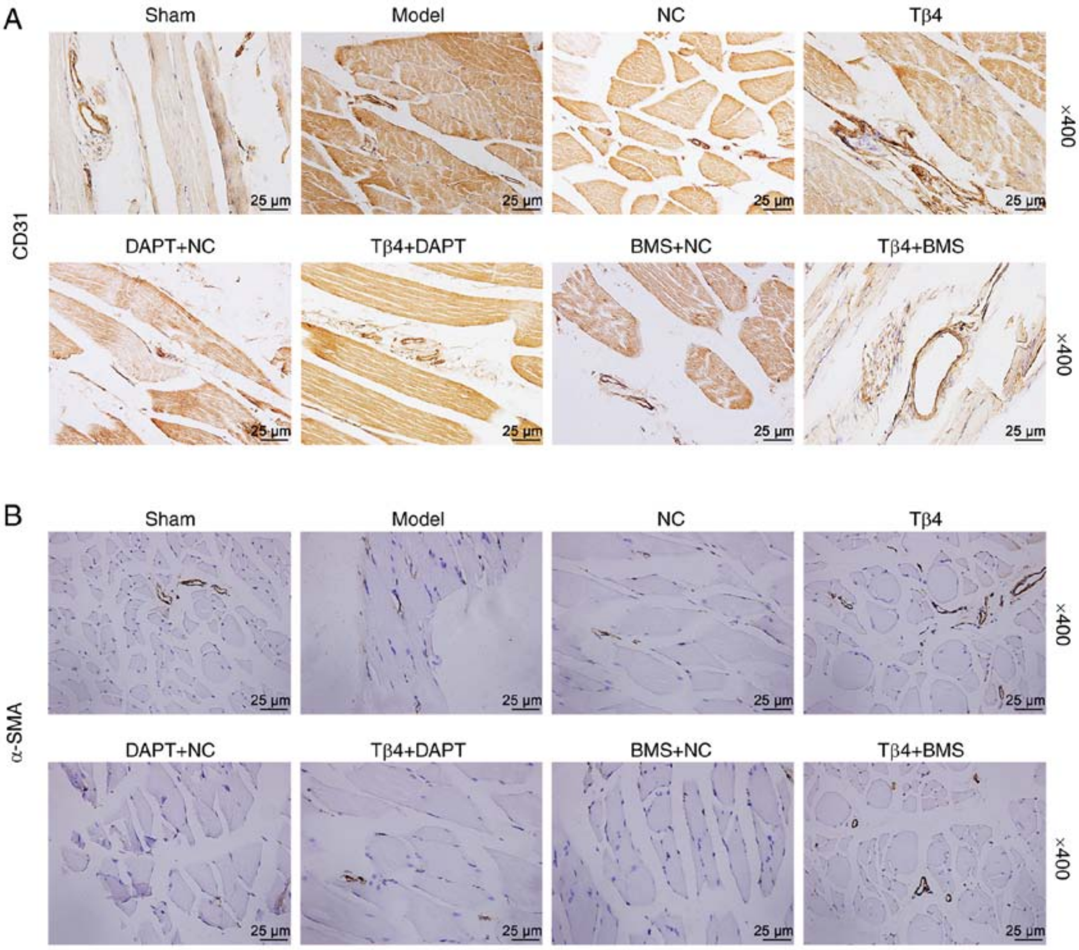

Figure 6. Tβ4 enhanced the capillary and arteriolar densities by regulating Notch/NF-κB signaling pathway in CLI mice. (A) Protein expression of CD31 was detected by immunohistochemistry in CLI mice muscle tissues. (B) Protein expression of α-SMA was detected by immunohistochemistry in CLI mice muscle tissues. All experiments were conducted three times. NC, negative control; Tβ4, thymosin-β 4; CLI, critical limb ischemia; α-SMA, α-smooth muscle actin.

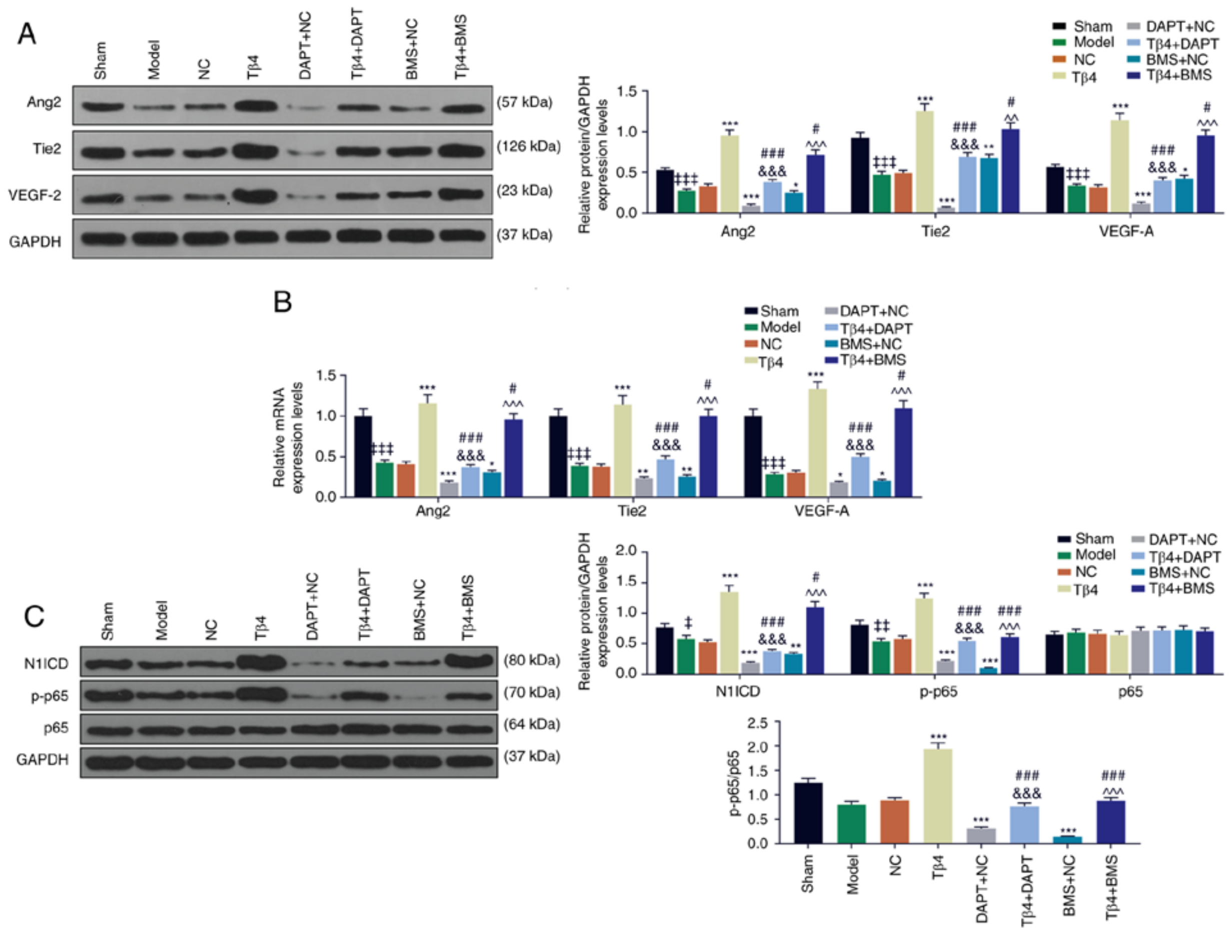

Figure 7. Tβ4 enhanced the expression of angiogenesis-related proteins by regulating Notch/NF-κB signaling pathway in CLI mice. (A) Protein expression of Ang2, tie2 and VEGF-A was detected by western blotting in CLI mice muscle tissues. GAPDH was used as an internal control. (B) mRNA expression of Ang2, tie2 and VEGF-A was detected by reverse transcription quantitative PCR in CLI mice muscle tissues. GAPDH was used as an internal control. (C) Protein expression of N1ICD, p-p65 and p65 was detected by western blotting in CLI mice muscle tissues. GAPDH was used as an internal control. All experiments were conducted three times. ‡P<0.05, ‡‡P<0.01 and ‡‡‡P<0.001 vs. Sham; *P<0.05, **P<0.01 and ***P<0.001 vs. NC; #P<0.05 and ###P<0.001 vs. Tβ4; &&&P<0.001 vs. DAPT + NC; ^^P<0.01 and ^^^P<0.001 vs. BMS + NC. VEGF-A, vascular endothelial growth factor A; Ang2, angiopoietin-2; tie2, tyrosine kinase 2; NC, negative control; N1ICD, NOTCH1 intracellular domain; Tβ4, thymosin-β 4; CLI, critical limb ischemia.

Tβ4 and DAPT + NC or BMS + NC groups (P<0.05, P<0.01 and P<0.001, respectively). Regarding the expressions of key proteins of Notch/NF-κB signaling pathway (Fig. 7C), the results demonstrated that expression of N1ICD, p-p65 and the ratio of p-p65/p65 were significantly increased by Tβ4, but were decreased following treatment with DAPT and BMS compared with the NC group (P<0.001). Furthermore, in Tβ4 + DAPT and Tβ4 + BMS groups, the promotion effects of Tβ4 on the expression of these proteins were reversed by DAPT and BMS treatment, compared with Tβ4 and DAPT + NC or BMS + NC groups (P<0.001). These findings suggested that Tβ4 had the ability to enhance angiogenesis by regulating Notch/NF-κB signaling pathway in CLI mice.

Discussion

Therapeutic angiogenesis and arteriogenesis remain important therapeutic goals in patients with CLI without revascularization possibilities. Numerous therapies have been attempted, with some encouraging effects (24-26). The present study aimed to explore the underlying mechanisms and pro-angiogenic effects of Tβ4 in CLI mice. The effects of Tβ4 on HUVEC were first investigated, and the results demonstrated Tβ4 could promote the migratory ability and angiogenesis of HUVEC, which were mediated by Notch/NF-κB signaling pathway. Furthermore, a CLI mice model was established followed by treatment with Tβ4 overexpression vector, the inhibitor of Notch pathway DAPT and the inhibitor of NF-κB pathway BMS. The results further demonstrated that Tβ4 could increase the capillary and arteriolar densities in CLI mice muscle tissues by regulating Notch/NF-κB signaling pathway. These findings suggested that Tβ4 may promote angiogenesis in CLI mice via regulation of Notch/NF-κB pathway.

Tβ4 was first isolated from the thymus and belongs to the β-thymosin family, which consists of several structurally related amino acid polypeptides (27). Tβ4 lacks a secretion signal, therefore it is speculated that its presence in body fluids might be due to damaged cell (10,27,28). Tβ4 was reported to take part in tissue damage-related diseases, such as dermal injuries, cerebral ischemia-reperfusion injury, heart injury and CLI (14,15,28-30). Furthermore, during tissue injury, Tβ4 can promote endothelial cell migration and tube formation (10,12). Similarly, the present study demonstrated that Tβ4 may stimulate the migratory ability and tube formation of HUVEC. In addition, this study demonstrated that Tβ4 could increase the capillary and arteriolar densities of CLI mice muscle tissues. These findings suggested that Tβ4 may have the ability to induce angiogenesis in CLI mice.

Previous studies reported that Ang-tie signaling is an important regulator signal in vascular development, angiogenesis and remodeling (31,32). In the Ang family, Ang2 is usually secreted in diseased or remodeling vessels and has been identified as the main ligand for tie2 (31,33). Tie2 plays a central role in promoting vascular stability, and therapeutic drugs that target the Ang-tie signaling axis to enhance tie2 activation have been extensively explored in ischemic vascular diseases, various types of cancer and inflammation (31,32). The expression of Ang2 and tie2 in HUVEC and CLI mice muscle tissues following Tβ4 overexpression was therefore determined in the present study. The results demonstrated that Tβ4 upregulated the expression of Ang2 and Tie2 in both HUVEC and CLI mice muscle tissues, which further confirmed previous results. In addition, VEGFA is one vascular endothelial growth factor, which has been strongly associated with angiogenesis in endothelial cells (34,35). In the present study, the expression of VEGFA was therefore evaluated and the results demonstrated that Tβ4 also increased VEGFA expression, which confirmed that Tβ4 could induce angiogenesis in CLI mice.

Previous studies have reported that Notch/NF-κB signaling pathway is highly related to the process of angiogenesis (36-40). Notch1 is part of the Notch family that regulates cell fate and VEGF expression in various types of cell, including HUVEC (10,39,41). Once ischemia occurrs, Notch1 would bind to its ligands (Jagged1 or Jagged2, or Delta-like 1, 3, or 4) to form a dimer and cleaved into N1CID, leading to VEGFA overexpression (42,43). Previous studies reported that activation of Notch signaling pathway could also promote NF-κB pathway following ischemia (40). After ischemia onset, Notch induces free NF-κB to translocate into the nucleus and to activate the expression of pro-angogenic factors, such as VEGFA, leading to angiogenesis of endothelial cell (37,40,44). The present study hypothesized therefore that Notch/NF-κB signaling pathway could be involved in the process of Tβ4-induced angiogenesis. After inhibiting Notch and NF-κB signaling pathway, the results demonstrated that Notch/NF-κB pathway might be related to Tβ4-induced angiogenesis.

In conclusion, the presents tudy demonstrated that Tβ4 may induce angiogenesis in CLI mice by regulating Notch/NF-κB signaling pathway, and may be considered as a therapeutic target for CLI treatment. However, whether Tβ4 could induce angiogenesis in a clinical setup requires further investigation focusing on application, duration, dosage and safety of Tβ4 treatment.

Acknowledgements

Not applicable.

Funding

No funding was received.

Availiability of data and materials

The datasets used and/or analyzed during the current study are available from the corresponding author on reasonable request.

Authors' contributions

SL and HC made substantial contributions to the conception and design of the study. YX, JD, XR and LZ were involved in data acquisition, analysis and interpretation. SL and HC were responsible for drafting the article and critically revising it for important intellectual content. All authors agreed to be accountable for all aspects of the work, in ensuring that questions related to the accuracy or integrity of the work were appropriately investigated and resolved. All authors read and approved the final manuscript.

Ethics approval and consent to participate

This study was approved by the Committee of Experimental Animals of The First Affiliated Hospital of Zhejiang Chinese Medical University (approval no. Z20190312G).

Patient consent for publication

Not applicable.

Competing interests

The authors declare that they have no competing interests.

References

1. Conte SM and Vale PR: Peripheral arterial disease. Heart Lung Circ 27: 427-432, 2018.
2. Nehler MR, Duval S, Diao L, Annex BH, Hiatt WR, Rogers K, Zakharyan A and Hirsch AT: Epidemiology of peripheral arterial disease and critical limb ischemia in an insured national population. J Vasc Surg 60: 686-695 e682, 2014.
3. Dua A and Lee CJ: Epidemiology of peripheral arterial disease and critical limb ischemia. Tech Vasc Interv Radiol 19: 91-95, 2016.
4. Albrecht-Schgoer K, Barthelmes J, Schgoer W, Theurl M, Nardin I, Lener D, Gutmann C, Dünnhaupt S, Bernkop-Schnürch A and Kirchmair R: Nanoparticular delivery system for a secretoneurin derivative induces angiogenesis in a hind limb ischemia model. J Control Release 250: 1-8, 2017.
5. Constantinescu IM, Bolfa P, Constantinescu D, Mironiuc AI and Gherman CD: Treatment with sildenafil and donepezil improves angiogenesis in experimentally induced critical limb ischemia. Biomed Res Int 2017: 9532381, 2017.
6. Ishibashi T and Ryan SJ: Maturation of newly-formed subretinal vessels. EXS 61: 59-63, 1992.
7. Zhao C, Wang X, Zhao Y, Li Z, Lin S, Wei Y and Yang H: A novel xenograft model in zebrafish for high-resolution investigating dynamics of neovascularization in tumors. PLoS One 6: e21768, 2011.
8. Sajib S, Zahra FT, Lionakis MS, German NA and Mikelis CM: Mechanisms of angiogenesis in microbe-regulated inflammatory and neoplastic conditions. Angiogenesis 21: 1-14, 2018.
9. Vasilopoulou E, Riley PR and Long DA: Thymosin-β4: A key modifier of renal disease. Expert Opin Biol Ther 18: 185-192, 2018.
10. Lv S, Cheng G, Zhou Y and Xu G: Thymosin β4 induces angiogenesis through Notch signaling in endothelial cells. Mol Cell Biochem 381: 283-290, 2013.
11. Sanders MC, Goldstein AL and Wang YL: Thymosin beta 4 (Fx peptide) is a potent regulator of actin polymerization in living cells. Proc Natl Acad Sci USA 89: 4678-4682, 1992.
12. Kobayashi T, Okada F, Fujii N, Tomita N, Ito S, Tazawa H, Aoyama T, Choi SK, Shibata T, Fujita H and Hosokawa M: Thymosin-beta4 regulates motility and metastasis of malignant mouse fibrosarcoma cells. Am J Pathol 160: 869-882, 2002.
13. Renga G, Oikonomou V, Stincardini C, Pariano M, Borghi M, Costantini C, Bartoli A, Garaci E, Goldstein AL and Romani L: Thymosin β4 limits inflammation through autophagy. Expert Opin Biol Ther 18 (Suppl 1): S171-S175, 2018.

14. Kleinman HK and Sosne G: Thymosin β4 promotes dermal healing. Vitam Horm 102: 251-275, 2016.
15. Trenkwalder T, Deindl E, Bongiovanni D, Lee S, Schunkert H, Kupatt C and Hinkel R: Thymosin-β4-mediated therapeutic neovascularization: Role of the PI3K/AKT pathway. Expert Opin Biol Ther 15 (Suppl 1): S175-S185, 2015.
16. Quan Z, Wang QL, Zhou P, Wang GD, Tan YZ and Wang HJ: Thymosin β4 promotes the survival and angiogenesis of transplanted endothelial progenitor cells in the infarcted myocardium. Int J Mol Med 39: 1347-1356, 2017.
17. Zhao Y, Song J, Bi X, Gao J, Shen Z, Zhu J and Fu G: Thymosin β4 promotes endothelial progenitor cell angiogenesis via a vascular endothelial growth factor-dependent mechanism. Mol Med Rep 18: 2314-2320, 2018.
18. Zhao J, Liang Y, Song F, Xu S, Nian L, Zhou X and Wang S: TSG attenuates LPC-induced endothelial cells inflammatory damage through notch signaling inhibition. IUBMB Life 68: 37-50, 2016.
19. MacMaster JF, Dambach DM, Lee DB, Berry KK, Qiu Y, Zusi FC and Burke JR: An inhibitor of IkappaB kinase, BMS-345541, blocks endothelial cell adhesion molecule expression and reduces the severity of dextran sulfate sodium-induced colitis in mice. Inflamm Res 52: 508-511, 2003.
20. Grimaldo S, Tian F and Li LY: Sensitization of endothelial cells to VEGI-induced apoptosis by inhibiting the NF-kappaB pathway. Apoptosis 14: 788-795, 2009.
21. Burke JR, Pattoli MA, Gregor KR, Brassil PJ, MacMaster JF, McIntyre KW, Yang X, Iotzova VS, Clarke W, Strnad J, *et al*: BMS-345541 is a highly selective inhibitor of I kappa B kinase that binds at an allosteric site of the enzyme and blocks NF-kappa B-dependent transcription in mice. J Biol Chem 278: 1450-1456, 2003.
22. Peng X, Zhou J, Li B, Zhang T, Zuo Y and Gu X: Notch1 and PI3K/Akt signaling blockers DAPT and LY294002 coordinately inhibit metastasis of gastric cancer through mutual enhancement. Cancer Chemother Pharmacol 85: 309-320, 2020.
23. Schmittgen TD and Livak KJ: Analyzing real-time PCR data by the comparative C(T) method. Nat Protoc 3: 1101-1108, 2008.
24. Farber A and Eberhardt RT: The current state of critical limb ischemia: A systematic review. JAMA Surg 151: 1070-1077, 2016.
25. Falluji N and Mukherjee D: Critical and acute limb ischemia: An overview. Angiology 65: 137-146, 2014.
26. Liew A, Bhattacharya V, Shaw J and Stansby G: Cell therapy for critical limb ischemia: A meta-analysis of randomized controlled trials. Angiology 67: 444-455, 2016.
27. Sosne G, Qiu P, Goldstein AL and Wheater M: Biological activities of thymosin beta4 defined by active sites in short peptide sequences. FASEB J 24: 2144-2151, 2010.
28. Yang WS, Kang S, Sung J and Kleinman HK: Thymosin β4: Potential to treat epidermolysis bullosa and other severe dermal injuries. Eur J Dermatol 29: 459-467, 2019.
29. Zhang Z, Liu S and Huang S: Effects of thymosin β4 on neuronal apoptosis in a rat model of cerebral ischemiareperfusion injury. Mol Med Rep 20: 4186-4192, 2019.
30. Bjørklund G, Dadar M, Aaseth J and Chirumbolo S: Thymosin β4: A multi-faceted tissue repair stimulating protein in heart injury. Curr Med Chem: July 31, 2019 (Epub ahead of print).
31. Zhang Y, Kontos CD, Annex BH and Popel AS: Angiopoietin-tie signaling pathway in endothelial cells: A computational model. iScience 20: 497-511, 2019.
32. Saharinen P, Eklund L and Alitalo K: Therapeutic targeting of the angiopoietin-TIE pathway. Nat Rev Drug Discov 16: 635-661, 2017.
33. Thurston G and Daly C: The complex role of angiopoietin-2 in the angiopoietin-tie signaling pathway. Cold Spring Harb Perspect Med 2: a006550, 2012.
34. Perez-Moral N, Needs PW, Moyle CWA and Kroon PA: Hydrophobic interactions drive binding between vascular endothelial growth factor-A (VEGFA) and polyphenolic inhibitors. Molecules 24: 2785, 2019.
35. Bhisitkul RB: Vascular endothelial growth factor biology: Clinical implications for ocular treatments. Br J Ophthalmol 90: 1542-1547, 2006.
36. Shukla K, Sonowal H, Saxena A and Ramana KV: Didymin by suppressing NF-κB activation prevents VEGF-induced angiogenesis in vitro and in vivo. Vascul Pharmacol 115: 18-25, 2019.
37. Huang DY, Dai ZR, Li WM, Wang RG and Yang SM: Inhibition of EGF expression and NF-κB activity by treatment with quercetin leads to suppression of angiogenesis in nasopharyngeal carcinoma. Saudi J Biol Sci 25: 826-831, 2018.
38. Si W, Xie W, Deng W, Xiao Y, Karnik SS, Xu C, Chen Q and Wang QK: Angiotensin II increases angiogenesis by NF-κB-mediated transcriptional activation of angiogenic factor AGGF1. FASEB J 32: 5051-5062, 2018.
39. Li L, Tang P, Zhou Z, Wang Q, Xu T, Zhao S, Huang Y, Kong F, Liu W, Cheng L, *et al*: GIT1 regulates angiogenic factor secretion in bone marrow mesenchymal stem cells via NF-κB/notch signalling to promote angiogenesis. Cell Prolif 52: e12689, 2019.
40. Xu D, Xia N, Hou K, Li F, Chen S, Hu Y, Fang W and Li Y: Clematichinenoside facilitates recovery of neurological and motor function in rats after cerebral ischemic injury through inhibiting notch/NF-κB pathway. J Stroke Cerebrovasc Dis 28: 104288, 2019.
41. Saito T and Tanaka S: Molecular mechanisms underlying osteoarthritis development: Notch and NF-κB. Arthritis Res Ther 19: 94, 2017.
42. Chen Y, Zhao B, Zhu Y, Zhao H and Ma C: HIF-1-VEGF-notch mediates angiogenesis in temporomandibular joint osteoarthritis. Am J Transl Res 11: 2969-2982, 2019.
43. Luo Z, Shang X, Zhang H, Wang G, Massey PA, Barton SR, Kevil CG and Dong Y: Notch signaling in osteogenesis, osteoclastogenesis, and angiogenesis. Am J Pathol 189: 1495-1500, 2019.
44. Huang F, Yao Y, Wu J, Liu Q, Zhang J, Pu X, Zhang Q and Xia L: Curcumin inhibits gastric cancer-derived mesenchymal stem cells mediated angiogenesis by regulating NF-κB/VEGF signaling. Am J Transl Res 9: 5538-5547, 2017.